Running Head: Load Dependent Neural Systems

Functional Connectivity Reveals Load Dependent Neural Systems Underlying Encoding and Maintenance in Verbal Working Memory

Todd S. Woodward[1,2]

Tara A. Cairo[1]

Christian C. Ruff[3]

Yoshio Takane[4]

Michael A. Hunter[5]

&

Elton T. C. Ngan[6]

[1] Department of Research, Riverview Hospital, Coquitlam, Canada
[2] Department of Psychology, Simon Fraser University, Burnaby, Canada
[3]Institute of Cognitive Neuroscience, University College, London, United Kingdom
[4]Department of Psychology, McGill University, Montreal, Canada
[5]Department of Psychology, University of Victoria, Victoria, Canada
[6] Department of Psychiatry, University of British Columbia, Vancouver, Canada

Author Notes:
Please address all correspondence to: Todd S. Woodward, Ph.D., Room 105, Department of Research, Administration Building, Riverview Hospital, 2601 Lougheed Highway, Coquitlam, B.C., Canada, V3C 4J2. E-mail: toddswoodward@gmail.com. Phone: 604-524-7697. Fax: 604-524-7137.

ABBREVIATIONS

SIRT - Sternberg item recognition test

CPCA - constrained principal component analysis

PCA - principal component analysis

BA - Brodmann's area

FIR - finite impulse response

HR - hemodynamic response

EPI - echo-planar images

GRE - gradient echo

BOLD - blood oxygen-level dependent

ITI - inter trial interval

fMRI - functional magnetic resonance imaging

ACC - anterior cingulate cortex

VLPFC - ventrolateral prefrontal cortex

ABSTRACT

One of the main challenges in working memory research has been to understand the degree of separation and overlap between the neural systems involved in encoding and maintenance. In the current study we used a variable load version of the Sternberg item recognition test (SIRT; 2, 4, 6, or 8 letters) and a functional connectivity method based on constrained principal component analysis (CPCA) to extract load-dependent neural systems underlying encoding and maintenance, and to characterize their anatomical overlap and functional interaction. Based on the pattern of functional connectivity, CPCA identified a load-dependent encoding system comprising bilateral occipital (BA 17, 18), bilateral superior parietal (BA 7), bilateral dorsolateral prefrontal (BA 46), and dorsal anterior cingulate (BA 24, 32) regions. For maintenance, in contrast, CPCA identified a system that was characterized by both load-dependent increases and decreases in activation. The structures in this system jointly activated by maintenance load involved left posterior parietal (BA 40), left inferior prefrontal (BA 44), left premotor and supplementary motor areas (BA 6), and dorsal cingulate regions (BA 24, 32), while the regions displaying maintenance-load-dependent activity decreases involved bilateral occipital (BA 17, 18), posterior cingulate (BA 23) and rostral anterior cingulate/orbitofrontal (BA 10, 11, 32) regions. The correlation between the encoding and maintenance systems was strong and negative (Pearson's r = -.55), indicting that some regions important for visual processing during encoding displayed reduced activity during maintenance, while subvocal rehearsal and phonological storage regions important for maintenance showed a reduction in activity during encoding. In summary, our analyses suggest that separable and complementary subsystems underlie encoding and maintenance in verbal working memory, and they demonstrate how CPCA can be employed to characterize neuronal systems and their functional contributions to higher-level cognition.

WORDS: WORKING MEMORY; FUNCTIONAL CONNECTIVITY; ENCODING; MAINTENANCE; PRINCIPAL COMPONENT ANALYSIS; PHONOLOGICAL LOOP

Functional Connectivity Reveals Load Dependent Neural Systems Underlying Encoding and Maintenance in Verbal Working Memory

Working memory allows individuals to maintain and manipulate a limited amount of information in an active state for a brief period of time. It can operate on a variety of cognitive representations, such as tastes, sounds, images, phonemes, concepts, locations, patterns, and colors (Baddeley, 1992). In the current study we focus on the encoding and maintenance of phonological information, often referred to as verbal working memory. Functional imaging studies of verbal working memory typically investigate the maintenance phase (D'Esposito et al., 1999, Postle et al., 2000), but more recently efforts have been focussed on studying both encoding and maintenance simultaneously (D'Esposito et al., 2000, Manoach et al., 2003, Cairo et al., 2004, Narayanana et al., 2005). However, due to their temporal adjacency and fixed order, determination of the degree of separation and overlap between the neural systems involved in encoding and maintenance remains a challenge. The focus of the current study was to demonstrate how multivariate statistical methodology can identify separable neuronal subsystems underlying encoding and maintenance, and further characterize their functional contribution to these two phases of working memory.

One method of separating the neural systems involved in encoding from those involved in maintenance involves selectively modeling only the later portion of maintenance (Rypma and D'Esposito, 1999, p. 6559, Rypma and D'Esposito, 2000). While this strategy minimizes the risk of misattributing encoding related activity to maintenance, it has the reverse effect of increasing the misattribution of early maintenance activity to encoding. Moreover, this approach does not take into consideration the adverse effects of multicolinearity on regression models (see Cairo et al., 2004, for a discussion of these issues). A different approach to studying maintenance involves interpreting the average finite impulse responses (FIR) for working memory blocks, with maintenance-free blocks (i.e., no delay) differenced out

(Manoach et al., 2003). Although this approach avoids the adverse effects of multicolinearity associated with regression models, late activity from encoding (possibly disrupted by the probe in the "no delay" control condition) may still be misattributed to the maintenance phase.

Both the regression and subtraction approaches, by definition, forfeit exploration of potential functional relationships between the neural systems underlying encoding and maintenance aspects of working memory. For example, regression weights do not reflect variance in activation that is shared between the conditions of interest; moreover, subtraction methodologies difference out neural systems that contribute to both encoding and maintenance. Moreover, both the aforementioned methods are based on multiple univariate null-hypothesis tests; this contrasts with analyses that examine functional connectivity between regions, which provide information about regions that are determined by correlation of their activity with other voxels (Friston et al., 1997, Lin et al., 2003, McIntosh et al., 2004, Viviani et al., 2005).

In the current study, we used a multivariate technique that allows the simultaneous extraction of overlapping but distinct neural systems for encoding and maintenance, based on analysis of functional connectivity. This method of analysis is a special application of constrained principal component analysis (CPCA), which greatly reduces the multicolinearity concerns associated with the multiple univariate null-hypothesis tests, because it does not involve interpretation of regression weights. Instead, CPCA uses singular value decomposition (SVD) of the functional activations, with the variance constrained to the experimental conditions of interest. This application of SVD is essentially identical to the eigendecomposition that forms the basis of principal component analysis (PCA; Jolliffe, 2002), and we will use the eigenvalue/eigenvector terminology in order to maintain consistency with the PCA literature. As with PCA, CPCA involves interpretation of eigenvectors (i.e., component weights or loadings) instead of regression weights. Importantly, CPCA allows investigation of memory load, because the separable neural systems underlying encoding and maintenance should display load dependence for their respective conditions on the resultant components. The simultaneous extraction of separate load-dependent neural

systems for both encoding and maintenance, and computation of functional interaction between these systems, is not possible using traditional methods of analysis.

We utilized a Sternberg item recognition test (SIRT) with varying levels of load. The SIRT requires subjects to memorize a short list of stimuli, maintain this information in an active state over a brief delay, and then use this information to indicate if a probe is or is not part of the memorized list. A conventional regression-based analysis of the currently analyzed data has been published (Cairo et al., 2004), and several design parameters were adjusted to ensure that the multicolinearity between the phases was low, avoiding redundancy in the conditions of interest. However, in our previous analysis, careful consideration of multicolinearity led to the inability to selectively model load for maintenance, because separating the maintenance component into fine distinctions led to high correlations between encoding and maintenance covariates of the same load. The current method of analysis overcame these limitations (and others mentioned above), greatly clarifying the functional interaction of load-dependent working memory systems for encoding and maintenance.

METHOD

Participants

The sample consisted of 18 right handed, healthy, native English speakers (10 women, mean age = 27.50 years, age range = 18 - 35) who were recruited by advertisement and word of mouth from the community of Vancouver, British Columbia, and outlying regions. All participants were right-handed, had no personal history of mental illness or neurological conditions, no generalized medical conditions requiring treatment, no family history of any psychotic disorder, and no contraindication for MR scanning. All subjects had 20/20 or corrected to 20/20 vision. Participants underwent screening for MRI compatibility and gave their written consent. The procedures administered complied with University ethical approval.

Materials

Eighteen sets of each of 2, 4, 6 or 8 differing capitalized consonants were prepared in Times New Roman 38 point font for the encoding condition (encoding letter string). The combination of consonants for each screen display was determined by random selection without replacement. An additional set of single lowercase consonants (test letters) were prepared for the retrieval phase, such that this consonant either matched or did not match one of the consonants in the encoding condition. The probability of the test letter having been in the encoded letter string was 0.5. A "+" sign in the same font was displayed during the ISI, and the word "RELAX" in the same font was presented during blank trials.

Apparatus

Echo-planar images (EPI) were collected on a standard clinical GE 1.5 T system fitted with a Horizon Echo-speed upgrade. Conventional spin-echo T1 weighted capital localizers were used to view the positioning of the participant's head and to graphically prescribe the functional image volumes. Functional image volumes were collected with a gradient echo (GRE) sequence (TR/TE 3000/40 ms, 90 flip angle, FOV 24 X 24 cm, 64 X 64 matrix, 62.5 kHz bandwidth, 3.75 X 3.75 mm in plane resolution, 5.00 mm slice thickness, 29 slices, 145 mm axial brain coverage). This sequence is sensitive to the blood oxygen-level dependent (BOLD) contrast. Each stimulus run consisted of 196 scans (encompassing the entire brain). The first 12 s collected at the beginning of each run were discarded, to avoid variation due to T1 saturation effects.

Stimuli were presented on a personal computer with Presentation software (Neurobehavioral Systems, 2001). Stimuli were projected from an LCD projector onto a screen mounted at the foot of the MRI table. An angled mirror reflected stimuli from the screen into the participants' field of view. Responses were recorded via a fiber-optic response device (Lightwave Medical, Vancouver, BC).

Procedure and Task Design

A trial consisted of presentation of the encoding letter string for 4 s (encoding phase), a delay of

3, 4 or 5 s (counterbalanced across conditions; maintenance phase), and a display of a test letter for 1s. Subjects were required to indicate if a single consonant in lowercase presented for 1s after this delay was the same as one of the encoding letters or different from all of the encoding letters. “Same” and “Different” responses were indicated by index and middle finger presses, and the finger-response assignments were counterbalanced across subjects. This rapid presentation design allowed each of the four memory load condition to be presented 18 times. The ITI was jittered (3, 4 or 5 seconds), and during the ITI a “+” was displayed starting 1s after the test letter and ending 1s before the encoding letters. Eighteen additional blank trials (20% of total trials) were also included, during which the word RELAX was presented. The jittering and inclusion of blank trials were introduced to produce temporal shift in stimulus presentation across the TR interval (see Cairo et al., 2004 for a more detailed explanation of this approach and the rationale for reducing multicolinearity).

Before entering the scanner, subjects were given the instructions for the task and 10 practice trials with varying memory loads. Participants were told that they would see uppercase letters presented on the screen, and that after a short delay one lowercase letter would follow. They were instructed to attend to the uppercase letters, and to indicate if the lowercase letter presented after the delay was one of the previously viewed uppercase letters. When in the scanner, the instructions were repeated, and the run lasted just under 10 minutes.

Processing and Analysis

Image Processing

Functional images were reconstructed offline. Statistical Parametric Mapping software (SPM99—Wellcome Institute of Cognitive Neurology, London, UK) was used for image realignment, normalization into Talairach stereotaxic anatomical space (using affine and non-linear components, as implemented in SPM99), and smoothing using a Gaussian kernel (8 mm FWHM) to compensate for intersubject anatomical differences, and to optimize the signal to noise ratio. The images were filtered

with a high pass filter (cut-off period 89 s) to remove noise associated with low frequency confounds (e.g. respiratory artefact). A notch filter (at the Nyquist frequency, with a period of 6 s) was also applied to remove noise associated with alternations of the applied radio frequency field.

Design Matrix

The values in the design matrix are synthetic HR functions formed by summing two gamma functions, as is implemented in SPM99 (Friston et al., 1994, Friston et al., 1998). For each scan series, the model of the composite HR for the entire run comprises a sequence of appropriately placed synthetic HRs to each encoding and maintenance load. Encoding was modeled as the convolution of a 4-s box-car (beginning at the onset of the encoding letters), and maintenance was modeled as the convolution of a 3-, 4- or 5-s boxcars (corresponding to the duration of the delay) with the synthetic HR. Thus, the design matrix created by SPM99 consisted of one row for each of the 3528 scans (18 subjects X 196 scans), and one column for each of the 162 conditions (18 subjects X 8 conditions + 18 constant terms). Synthetic HRs for the response phases were not included in the design matrix; therefore, the variance in BOLD signal that is attributable to the response phase was apportioned to the $GE*$ aspect of the external analysis (see below), and does not influence the components reported below.

Functional Connectivity Analysis

The Statistical Parametric Mapping (SPM) analysis of these data has been presented elsewhere (Cairo et al., 2004). The purpose of the functional connectivity analyses presented here was to separately identify load-dependent neural systems underlying encoding and maintenance, and to identify functional interactions between these two systems. Constrained principal component analysis (CPCA) (Takane and Hunter, 2001, Hunter and Takane, 2002) with promax rotation was used. This method allowed extraction of functionally interacting but distinct neural systems for encoding and maintenance; moreover, CPCA capitalized on the load dependent nature of the task, because separable neural systems underlying each sub-process should display load dependant activation for their respective condition, and CPCA allows

quantification of this pattern.

CPCA is a general method for structural analysis of multivariate data that combines regression analysis and principal component analysis into a unified framework. Applied to functional magnetic resonance imaging (fMRI) data, CPCA can identify components directly relevant to experimental conditions of interest by integrating this information prior to computation of components. As for typical PCA, this method derives eigenimages from singular-value decomposition of brain activation time series. However, in contrast with typical PCA methods, CPCA allows the separate analysis of portions of the overall variability, defined by contrasts of interest.

Consider a data matrix containing columns of fMRI time series data (Z). In its essence, CPCA involves performing PCA on partitions of Z. To utilize CPCA for most fMRI designs, three matrices must be prepared. The first matrix of interest contains columns of the subject-mean-corrected filtered, smoothed, and normalized activations for all voxels over all scans: Z. We will refer to this matrix as the *activation matrix*. The second matrix, G, is the *design matrix* created by SPM. It contains columns of synthetic HRs that would be predicted over scans for idealized voxels responding only to the particular types of stimuli presented in the experiment. The third matrix contains the experimental contrasts of interest: A. We refer to this matrix as the *contrast matrix*, and it contains as many columns as there are contrasts of interest relevant to the columns of the design matrix G.

For fMRI designs conceptualized as outlined above, the uniqueness of each CPCA analysis is driven by the characteristics of the A matrix. For the present investigation, the A matrix consisted of 8 columns, each coding a distinct load/phase combination. Specifically, the first column coded encoding load 2, the second encoding load 4, the third encoding load 6, the fourth encoding load 8, the fifth maintenance load 2, the sixth maintenance load 4, the seventh maintenance load 6, and the eighth maintenance load 8. In terms of numeric codes, based on the matrix multiplication of GA, in the first column a weight of 1 was assigned to the columns of G representing the synthetic HR for encoding load 2; therefore, 18 ones were entered into the column corresponding to each row that would be multiplied

by the encoding load 2 synthetic HR for each subject in *G*. Zeros were entered for all other rows, including the constant rows. The same procedure was followed for each phase/load combination. Thus, the *A* matrix consisted of 162 rows (one weight for each column of the design matrix *G*; 8 X 18 + 18 constants), and 8 columns (one for each load/phase combination).

The matrix equations that characterize CPCA take the activation, design and contrast matrices as input. As a first step, measured activations in *Z* are predicted from the idealized activations in *G*. In order to achieve this, a familiar least-squares linear regression is carried out, whereby the activation matrix is regressed on the design matrix:

$$Z = GC + E\,. \qquad (1)$$

This analysis yields condition-specific regression weights in the *C* matrix (i.e., regression weights specific to the experimental conditions). The condition-specific regression weights are often presented in traditional analyses as beta images. Next, variability in the condition-specific regression weights are predicted from the contrast matrix, that expresses the hypothesized higher order structure. In other words, the matrix of condition-specific regression weights is regressed on the contrast matrix, yielding a matrix of contrast-specific regression weights:

$$C = AW + E^*. \qquad (2)$$

The contrast-specific regression weights in *W* convey the relative importance of each contrast for each voxel-specific regression weight. The next two steps involve algebraic substitutions. First, the right side of Equation 2 is substituted into Equation 1:

$$Z = G(AW + E^*) + E\,, \qquad (3)$$

which expands to:

$$Z = GAW + GE^* + E\,. \qquad (4)$$

Using this methodology, the activation matrix *Z* is split into three independent sources of variability: activation variability predictable from the experimental contrasts (*GAW*), activation variability predictable from the stimulus presentations, but independent of the experimental contrasts

(*GE**), and activation variability not predictable from the stimulus presentations (*E*). This step involving partitioning the variability in *Z* is referred to as the *external analysis* (Hunter and Takane, 2002). The details on how to fit higher order structure models such that all of the decompositions are orthogonal to one another are presented elsewhere (Takane and Hunter, 2001).

The next step involves extracting a component (or components) that represents a system (or systems) of functionally interconnected voxel activations. This involves singular value decomposition of the activation variability predictable from the experimental contrast (*GAW*), and is referred to as the *internal analysis* (Hunter and Takane, 2002). The maximum number of extractable components is equal to the rank of *GAW*, which is the minimum row or column subscript of *A*:

$$UDV' = GAW\ . \qquad (5)$$

The *V* matrix contains eigenvectors, and each column can be mapped onto brain images that are traditionally referred to as eigenimages (Friston, 1997). The *U* matrix contains component scores, and the rows correspond to scans. In previous work, the columns of *U* have been referred to as the temporal eigenvectors (Friston, 1997). The weights applied to *GA* to create *U* are very helpful for interpreting the neural system represented by the component solution with respect to the experimental contrasts. Namely, they indicate the importance of each contrast represented in the *A* matrix to the brain system(s) represented by the component(s) (Hunter and Takane, 2002).

The implementation of a contrast matrix *A* coded as a column of ones for each condition of interest offers a powerful exploratory tool. In this special case, the matrix *GA* is simply the synthetic HRs of interest collapsed down into one matrix with no zero entries and no constant terms. This means that the weights applied to *GA* to create *U* can be interpreted directly as importance of each condition/load combination to the components. These weights, the predictor weights (Hunter and Takane, 2002), form the basis of interpretation of the factors with respect to the experimental conditions of interest.

For pedagogical purposes, we now briefly present the matrix equations for CPCA using the data for one subject in the current study. As was mentioned above, the full *A* matrix consisted of 162 rows

(one weight for each column of the design matrix *G*; 8 X 18 + 18 constants), and 8 columns (one for each phase/load combination). An *A* matrix reduced down to a single subject would have 9 rows and 8 columns (see Table 1), and the *G* matrix reduced down to a single subject (extracted directly from the SPM_fMRIDesMtx.mat file routinely produced by SPM99) would have 196 rows (for 196 scans) and 9 columns, eight for the synthetic HR models computed for each phase/load combination (encoding load 2, 4, 6, 8, and maintenance load 2, 4, 6, and 8), and one for the constant term. For this particular dataset, SPM99 determined that 24,642 voxels could be considered located in brain matter (coordinates extracted from the mask.img file routinely produced by SPM99). Therefore, if three components are extracted, the core CPCA equations for one subject, with matrix dimension information, are as follows:

$$ {}_{196}Z_{24642} = {}_{196}G_9 A_8 W_{24642} + {}_{196}G_9 E^*_{24642} + {}_{196}E_{24642} \ , \qquad (6) $$

$$ {}_{196}U_3 D_3 V_{24642} \approx {}_{196}G_9 A_8 W_{24642} \ . \qquad (7) $$

For clarity of presentation, the above example was based on one subject, but extension to multiple subjects is straight-forward. The results presented below are based on data from 18 subjects analyzed simultaneously.

CPCA is a very general technique with a wide variety of applications. For example, the internal analysis can be restricted to contrasts of interest, as well as to neural circuits of interest. CPCA is primarily descriptive; however, statistical inference (assessment of reliability, hypothesis testing, etc.) is possible (Hunter and Takane, 2002), and is currently in development for fMRI.

RESULTS

The maximum number of components extractable using the aforementioned *A* matrix was 8, because this is the rank of the *GAW* matrix. The percentage of variation in *GAW* accounted for by each of these eight components extracted from the internal analysis (i.e., SVD of *GAW*) was: 66.64, 21.35, 5.94, 2.13, 1.80, 1.26, 0.47, 0.41, suggesting extraction of 3 factors. The predictor weights for each component are listed in Table 2 and in Figure 2 and Figure 3. Component 1 showed clear load dependence for

encoding, but no importance for maintenance. Component 3 showed clear load dependence for maintenance, and moderate load dependence for encoding, but in the opposite direction. Component 2 was not interpretable with respect to the load manipulations, suggesting that some neural activity that was predictable from the stimulus presentations could not be categorized by the nature of the experimental conditions. This component suggested the presence of a general "stimulus processing" component, characterized by bilateral activations in the cerebellum and many other cortical regions typically observed as activated in neuroimaging studies (e.g., bilateral temporal, frontal, parietal and occipital regions), and will not be discussed further here.

The load-dependent encoding system (Component 1) was dominated by bilateral occipital (BA 17, 18), bilateral superior parietal (BA 7), bilateral dorsolateral prefrontal (BA 46), and dorsal anterior cingulate regions (BA 24, 32). This was a clear replication of the activations that were involved in encoding in a load dependent fashion using the traditional analysis (Cairo et al., 2004), and reflects regions thought to be involved in visual processing and top-down attentional modulation of posterior cortical activity (Ranganath et al., 2003). The maintenance system (Component 3) involved one subsystem that was activated by maintenance load, and another which showed decreases in activity that were related to load. The maintenance-activated subsystem involved left posterior parietal (BA 40), left inferior prefrontal (BA 44), left premotor and supplementary motor areas (BA 6), and dorsal cingulate (BA 24, 32) regions, corresponding well to the average-load activations observed in our traditional analysis of these data (Cairo et al., 2004), and reflecting regions thought to be involved in and the subvocal rehearsal and phonological storage regions referred to in the literature (Smith and Jonides, 1998, Baddeley, 2003). The load-dependent subsystem that decreased activation during maintenance involved bilateral occipital (BA 17, 18), posterior cingulate (BA 23) and rostral anterior cingulate/orbitofrontal (BA 10, 11, 23) regions. In addition to the negative loadings suggesting that some (primarily occipital) regions decreased activation, the moderate *negative predictor weights* for the encoding condition that can be observed for the maintenance component (Table 2, Component 3,

encoding rows) suggest that the aforementioned neural network involved in maintenance decreases activation during encoding in a load dependent fashion. Correspondingly, the correlation between the encoding and maintenance systems was negative (Pearson's r = -.55).

DISCUSSION

In the current working memory study we used a novel statistical model, based on CPCA, to extract separate load dependent neural systems for both encoding and maintenance in a single analysis. The load-dependent encoding system was dominated by visual processing and attentional regions, and the load-dependent maintenance system was dominated by subvocal rehearsal and phonological storage regions. In addition, the results demonstrated that visual encoding regions reduce activation during maintenance, and that the subvocal rehearsal and phonological storage regions important for maintenance reduce activation during encoding. Taken as a whole, the novel contribution of the CPCA analysis over and above our standard previous analysis of these data (Cairo et al., 2004) was: (1) simultaneous extraction of load-dependent encoding and maintenance systems, (2) confirmation that visual processing regions decrease activation during maintenance, (3) confirmation that subvocal rehearsal and phonological storage regions decrease activation during encoding, and (4) the observation that the neural systems underlying encoding and maintenance are negatively correlated in the context of these experimental parameters.

With respect to the encoding system, similar patterns have been identified in previous studies (Rypma and D'Esposito, 1999, Smith and Jonides, 1999, Manoach et al., 2003, Cairo et al., 2004). As in our original analysis (Cairo et al., 2004), the strongest activation was found in the occipital cortex where visual information is processed. Many of the same regions have been implicated in salient stimulus processing, an involuntary attentional mechanism that allows information that is most likely to be relevant to behaviour to be selected from the environment (Coull, 1998), including bilateral occipital and parietal regions.

The observed maintenance system replicated many of the activations thought to underlie components of verbal working memory system. The left-lateralized inferior parietal activation extended from the postcentral gyrus into BA 40 and 7. The left BA 40 and 7 are thought to subserve a phonological store (Paulesu et al., 1993, Smith and Jonides, 1998, Baddeley, 2003), and have also observed load dependent activity in some studies (Ravizza et al., 2004, Chen and Desmond, 2005, Kirschen et al., 2005). Other regions of activation (all of which were load dependent) were in the left inferior prefrontal (BA 44), left premotor and supplementary motor areas (BA 6), and dorsal cingulate regions (BA 24, 32). This largely replicated the average-load activations observed in our previous study (Cairo et al., 2004) and in the literature (Smith and Jonides, 1998, Baddeley, 2003), thought to underlie subvocal rehearsal and phonological storage.

The predictor weights and negative loadings that reflect a load-dependent, reciprocal relationship between the encoding and maintenance systems are unique to CPCA methodology, and could not be detected by traditional methods of analysis. Although CPCA has clearly provided new insights into the functional relationship between the encoding and maintenance systems in working memory, the interpretation of this reciprocal relationship is not straight forward. On one hand, this reciprocal activation may, wholly or partially, reflect the natural consequences of the time invariance of the working memory task, such that low activation in phase A is negatively correlated with time-locked relatively high activations in phase B, and *vice versa*. This interpretation fits the load-dependent negative loadings for the visual regions on the maintenance component, and the load-dependent negative predictor weights for the encoding conditions on the maintenance component.

However, an alternative interpretation of this reciprocity is that the neural systems underlying encoding and maintenance optimize by reciprocal suppression, and/or that each system employs suppression as well as activation as an integral aspect of its neural network. For example, the reduced occipital activation during maintenance may optimize phonological maintenance by facilitating the attentional switch from processing externally presented visual information to maintaining internally

represented phonological information, and a similar argument can be made for suppression of maintenance regions during encoding. Some evidence for such reciprocity can be found in the literature; for example, one study investigating prefrontal activation reported decreasing ventrolateral prefrontal cortex (VLPFC) activation with increasing load at encoding, combined with evidence for increasing VLPFC activation with increasing load at maintenance (Rypma et al., 2002). Given that the VLPFC has been identified as important for subvocal rehearsal (Smith and Jonides, 1998, Baddeley, 2003), this result is congruent with our findings.

From this perspective, the negative loadings of rostral and posterior anterior cingulate cortex (ACC) on the maintenance component are of interest. The ACC participates in a neural circuit that regulates both cognitive and emotional processing, with the dorsal ACC being involved in the processing of attentionally demanding cognitive information (Bush et al., 2000, Ruff et al., 2001, Woodward et al., in revision), and the rostral and posterior ACC in emotional processing (Drevets and Raichle, 1998, Bush et al., 2000, Maddock et al., 2003). It has been shown that during the performance of attentionally demanding cognitive tasks, activity increases in the dorsal ACC, but decreases reciprocally in the rostral ACC (Drevets and Raichle, 1998, Bush et al., 2000). Based on this literature, suppression of the rostral and posterior aspects on the ACC may be expected during the intensive, internal, attentionally demanding cognitive processing that characterizes the maintenance phase. Thus, the regions with negative loadings on the maintenance component that are not involved in encoding, such as rostral and posterior ACC, orbital frontal cortex, and inferior temporal regions, are likely candidates for a suppression-for-optimization role in the neural network underlying maintenance.

One of the most evident differences between the currently reported CPCA analysis and for traditional analyses of these data (Cairo et al., 2004) was that, whereas previously we observed occipital activations during maintenance, the CPCA analysis suggests that occipital regions in fact decrease activation during maintenance. One reason for this discrepancy is that, despite careful methodological adjustments designed to reduce multicolinearity, the regression methodology used in our previous

analysis may have resulted in misattribution of particularly strong encoding activations to the maintenance phase. If strong occipital activation that accompanies encoding extends beyond what is predicted by the synthetic HR for that condition, it will be explained by the (correlated) synthetic HR meant to capture maintenance operations. CPCA, on the other hand, does not rely on regression weights for interpretation of results, but instead is based on analysis of functionally coordinated activation. Basing interpretation on patterns of coordinated activation is optimal for describing the functional separation and overlap of neural systems.

In summary, CPCA allowed simultaneous extraction of load-dependent encoding and maintenance systems, and suggested a reciprocal relationship between the neural systems underlying each. The reciprocal relationships that are readily observable using SVD techniques such as CPCA are seldom described by standard methodologies. It is becoming clear, as evidenced by the ACC literature reported above (Drevets and Raichle, 1998, Bush et al., 2000), that the balance of activation achieved by reciprocal relationships between neural regions may be as important as pure activations for understanding the neural underpinnings of the cognitive architecture. As methodologies such as CPCA become more widely available (e.g., Lin et al., 2003, McIntosh et al., 2004, Viviani et al., 2005), the interest in studying the reciprocal interaction of neural systems may increase.

ACKNOWLEDGEMENTS

This research was supported by a grant from the Mind Foundation of BC. The authors would like to thank MR technicians Trudy Harris, Sylvia Rennenberg and Jennifer McCord for assistance with data collection.

REFERENCES

Baddeley, A., 1992. Working memory: The interface between memory and cognition. Journal of Cognitive Neuroscience. 4, 281-288.

Baddeley, A., 2003. Working memory: looking back and looking forward. Nature Reviews Neuroscience. 4, 829-839.

Bush, G., Luu, P. and Posner, M. I., 2000. Cognitive and emotional influences in anterior cingulate cortex. Trends in Cognitive Science. 4, 215-222.

Cairo, T. A., Liddle, P. F., Woodward, T. S. and Ngan, E. T. C., 2004. The influence of working memory load on phase specific patterns of cortical activity. Cognitive Brain Research. 21, 377-387.

Chen, S. H. and Desmond, J. E., 2005. Cerebrocerebellar networks during articulatory rehearsal and verbal working memory tasks. Neuroimage. 24, 332-338.

Coull, J. T., 1998. Neural correlates of attention and arousal: insights from electrophysiology, functional neuroimaging and psychopharmacology. Progress in Neurobiology. 55, 343-361.

D'Esposito, M., Postle, B. R., Ballard, D. and Lease, J., 1999. Maintenance versus manipulation of information held in working memory: an event-related fMRI study. Brain and Cognition. 41, 66-86.

D'Esposito, M., Postle, B. R. and Rypma, B., 2000. Prefrontal cortical contributions to working memory: evidence from event-related fMRI studies. Experimental Brain Research. 133, 3-11.

Drevets, W. C. and Raichle, M. E., 1998. Reciprocal suppression of regional cerebral flood flow during emotional versus higher cognitive processes: implications for interactions between emotion and cognition. Cognition and Emotion. 12, 353-385.

Friston, K., 1997. Eigenimages and multivariate analyses. SPM short course notes. Institute of Neurology, Wellcome Department of Cognitive Neurology, London, pp. Chapter 5.

Friston, K., Jezzard, P. and Turner, R., 1994. Analysis of functional MRI time-series. Human Brain

Mapping. 1, 153-171.

Friston, K. J., Buechel, C., Fink, G. R., Morris, J., Rolls, E. and Dolan, R. J., 1997. Psychophysiological and modulatory interactions in neuroimaging. Neuroimage. 6, 218-229.

Friston, K. J., Fletcher, P., Josephs, O., Holmes, A. P., Rugg, M. D. and Turner, R., 1998. Event-related fMRI: characterizing differential responses. NeuroImage. 7, 30-40.

Hunter, M. A. and Takane, Y., 2002. Constrained principal component analysis: Various applications. Journal of Educational and Behavioral Statistics. 27, 105-145.

Jolliffe, I. T., 2002. Principal Component Analysis: Second Edition. Springer-Verlag, New York.

Kirschen, M. P., Chen, S. H., Schraedley-Desmond, P. and Desmond, J. E., 2005. Load- and practice-dependent increases in cerebro-cerebellar activation in verbal working memory: an fMRI study. Neuroimage. 24, 462-472.

Lin, F. H., McIntosh, A. R., Agnew, J. A., Eden, G. F., Zeffiro, T. A. and Belliveau, J. W., 2003. Multivariate analysis of neuronal interactions in the generalized partial least squares framework: simulations and empirical studies. Neuroimage. 20, 625-642.

Maddock, R. J., Garrett, A. S. and Buonocore, M. H., 2003. Posterior cingulate cortex activation by emotional words: fMRI evidence from a valence decision task. Human Brain Mapping. 18, 30-41.

Manoach, D. S., Greve, D. N., Lindgren, K. A. and Dale, A. M., 2003. Identifying regional activity associated with temporally separated components of working memory using event-related functional MRI. Neuroimage. 20, 1670-1684.

McIntosh, A. R., Chau, W. K. and Protzner, A. B., 2004. Spatiotemporal analysis of event-related fMRI data using partial least squares. Neuroimage. 23, 764-775.

Narayanana, N. S., Prabhakarana, V., Bungea, S. A., Christoffa, K., Finea, E. M. and Gabrielia, J. D. E., 2005. The Role of the Prefrontal Cortex in the Maintenance of Verbal Working Memory: An Event-Related fMRI Analysis. Neuropsychology. 19, 223-232.

Neurobehavioral Systems, 2001. Presentation), .50 edn. Neurobehavioral Systems Inc, San Francisco.

Paulesu, E., Frith, C. D. and Frackowiak, R. S., 1993. The neural correlates of the verbal component of working memory. Nature. 362, 342-345.

Postle, B. R., Zarahn, E. and D'Esposito, M., 2000. Using event-related fMRI to assess delay-period activity during performance of spatial and nonspatial working memory tasks. Brain Research Protocols. 5, 57-66.

Ranganath, C., Johnson, M. K. and D'Esposito, M., 2003. Prefrontal activity associated with working memory and episodic long-term memory. Neuropsychologia. 41, 378-389.

Ravizza, S. M., Delgado, M. R., Chein, J. M., Becker, J. T. and Fiez, J. A., 2004. Functional dissociations within the inferior parietal cortex in verbal working memory. Neuroimage. 22, 562-573.

Ruff, C. C., Woodward, T. S., Laurens, K. R. and Liddle, P. F., 2001. The role of the anterior cingulate cortex in conflict processing: evidence from reverse Stroop interference. Neuroimage. 14, 1150-1158.

Rypma, B., Berger, J. S. and D'Esposito, M., 2002. The influence of working-memory demand and subject performance on prefrontal cortical activity. Journal of Cognitive Neuroscience. 14, 721-731.

Rypma, B. and D'Esposito, M., 1999. The roles of prefrontal brain regions in components of working memory: effects of memory load and individual differences. Proceedings of the National Academy of Sciences of the United States of America. 96, 6558-6563.

Rypma, B. and D'Esposito, M., 2000. Isolating the neural mechanisms of age-related changes in human working memory. Nature Neuroscience. 3, 509-515.

Smith, E. E. and Jonides, J., 1998. Neuroimaging analyses of human working memory. Proceedings of the National Academy of Sciences of the United States of America. 95, 12061-12068.

Smith, E. E. and Jonides, J., 1999. Storage and executive processes in the frontal lobes. Science. 283, 1657-1661.

Takane, Y. and Hunter, M. A., 2001. Constrained principal component analysis: A comprehensive theory. Applicable Algebra in Engineering, Communication and Computing. 12, 391-419.

Viviani, R., Gron, G. and Spitzer, M., 2005. Functional principal component analysis of fMRI data. Human Brain Mapping. 24, 109-129.

Woodward, T. S., Ruff, C. C. and Ngan, E. T. C., in revision. Anterior Cingulate Activation and Cognitive Flexibility: An fMRI Investigation of Task Switching. Cognitive Brain Research.

Table 1. Example *A* matrix that could be used for a single-subject CPCA analysis. This is presented for pedagogical purposes only. Extension to multiple subjects as was used in the reported CPCA analysis is straight-forward, but cannot be presented here due to space restrictions. The *A* matrix is referred to as the *contrast matrix*, and it contains as many columns as there are contrasts of interest relevant to the columns of the design matrix *G*. In terms of numeric codes, based on the matrix multiplication of *GA*, in the first column a weight of 1 would be multiplied into the column of *G* representing the synthetic HR for encoding load 2, and so on for each column of *A* and its corresponding row in *G*. Zeros are entered for the constant rows, because the data is already subject-mean-corrected. The implementation of a contrast matrix *A* coded as a column of ones for each condition of interest offers a powerful exploratory tool, such that the weights applied to *GA* to create *U* can be interpreted directly as importance of each condition/load combination to the components.

		Encoding				Maintenance			
G Matrix Columns		2	4	6	8	2	4	6	8
Encoding	2	1	0	0	0	0	0	0	0
	4	0	1	0	0	0	0	0	0
	6	0	0	1	0	0	0	0	0
	8	0	0	0	1	0	0	0	0
Maintenance	2	0	0	0	0	1	0	0	0
	4	0	0	0	0	0	1	0	0
	6	0	0	0	0	0	0	1	0
	8	0	0	0	0	0	0	0	1
Constant		0	0	0	0	0	0	0	0

Table 2. Predictor weights for each component from the CPCA analysis. Predictor weights are the weights applied to *GA* to create *U*, and with the *A* matrix utilized in the present study, these weights can be interpreted directly as the importance of each condition/load combination to the components.

Predictor Weights				
Condition		Component		
		1	2	3
Encoding	2 Letter	0.40	0.67	-0.25
	4 Letter	0.74	0.19	-0.44
	6 Letter	1.15	0.46	-0.76
	8 Letter	1.15	0.00	-0.57
Maintenance	2 Letter	0.01	0.52	0.20
	4 Letter	-0.12	0.03	0.44
	6 Letter	0.02	0.84	0.80
	8 Letter	-0.23	0.73	1.21

Table 3. Dominant 5% of loadings for the encoding and maintenance components. The region that houses the peak of the clusters of interest is named, but the Brodmann Areas (BAs) into which the clusters extend are also listed, and BAs that house the peak for each cluster are bolded, if applicable. For the maintenance component, positive and negative loadings are listed separately.

Region	Encoding*		Maintenance*			
Frontal	L Mid (4) R Mid (25) L Inf (4)	.21 [-36,32,28] **45**,46 .23 [36,32,32] 45,**46**,48 .20 [-44,28,20] 45,**48**	L Mid (4) R Mid (92) L Inf (121)	.07 [-36,48,12] **46** .10 [40,44,28] 44,45,**46**,48 .10 [-48,28,32] 6,**44**,45,48	L Inf (16) L Iorb (19)	-.09 [-56,24 ,4] **45** -.09 [-28,32,-20] 11,38, **47**
Insula			L Ins (64) R Ins (37)	.10 [-44,16,-8] 38,47,**48** .09 [36,20,4] 38,47,**48**		
Parietal	L Sup (230) R Sup (384)	.29 [-28,-64,52] 2,**7**,39,40,48 .31 [24,-68,52] 2,3,**7**,40,48	L PtC (401) R Inf (43)	.17 [-40,-28,56] 2,**3**,4,6,7,39,40,48 .09 [48,-48,44] 39,**40**		
Sensorimotor	L PrC (409) R PrC (390)	.34 [-52,-12,40] 3,**4**,6,43,44,48 .29 [32,-8,48] 3,4,**6**,43,44,48	L SMA (20)	.10 [-4,-12,56] **6**	L PrC (96) R PrC (150)	-.13 [-48,-16,36] **3**,4,43,48 -.15 [44,-12,40] 3,4,**6**,43,48
Cingulate	R SMA (251)	.30 [-4,8,52] **6**,24,32	L Med (158)	.15 [0,24,44] 6,8,24,**32**	L Med (396) L Pos (353)	-.16 [-8,52,-8] 8,9,**10**,11,32 -.15 [-4,-52,24] 17,18,**23**,26,30
Temporal	L Hip (5) R Hip (1)	.22 [-28 ,-32, 0] **37** .20 [28, -28, -4] **20**	L Mid (20) L Fus (12) R Fus (11)	.07 [-56,-48,8] **21**,22 .08 [-36,-52,-4] **37** .08 [32,-52,0] **37**	L Mid (5) L Inf (11) R Inf (10) R Hip (3)	-.08 [-60,-4,-16] **21** -.09 [-36,4,-36] 20,**36** -.07 [40,8,-40] **20** -.08 [20,-28,-4] **27**
Basal Ganglia	L Put (170) R Put (109)	.24 [-25,11,0] 11,**48** .26 [20,15,-8] 11,**48**			L Put (50) R Put (57) R Put (5)	-.08 [-24,12,0] 28,34,36,38,**48** -.09 [20,16,0] 11,28,34,**48** -.07 [32,-12,-4] **48**
Occipital	L Cun (527) R Lin (459)	.36 [-12, -96,-8] 7,**17**,18,19 .36 [12, -88,-8] 7,17,**18**,19			L Lin (307) R Lin (519)	-.18 [-36,-88,-16] 17,**18**,19,37 -.19 [24,-92,-12] 7,17,**18**,19,37
Cerebellar	L Pos (78) R Pos (119)	.23 [-28,-72,-28] .29 [12, -80,-20]	L Pos (12) R Ant (203) R Ant (17)	.09 [-32,-68,-40] .11 [24, -64, -32] 17,18,19,37 .09 [12,-36,-16]	L Ant (21) R Pos (29)	-.11 [-36,-40,-28] **37** -.11 [24,-80,-40]

*Location of peak (Extent); Loadings positive/negative; [MNI coordinate of peak: x,y,z]; Brodmann's Areas into which cluster extends, with peak area in bold. Abbreviations used to describe location of peak: Ant: Anterior; Cun: Cuneus; Fus: Fusiform; Hip: Hippocampus; Inf: Inferior; Ins: Insula; Iorb: Inferior orbital; Lin: Lingual; Med: Medial; Mid: Middle; Pos: Posterior; PrC: Precentral; PtC: Postcentral; Put: Putamen; SMA: Supplementary motor area; Sup: Superior.

FIGURE CAPTIONS

Figure 1. We employed a verbal working-memory task with encoding, maintenance, and retrieval epochs under four different load conditions. During a single trial of this task, subjects were presented with a string of 2, 4, 6 or 8 different letters which they were instructed to remember over a short delay. Subjects were required to indicate if a letter presented after the delay was the same as one of the remembered letters or different from all of the remembered letters. The delay and intertrial interval were both varied (3, 4 or 5 seconds) in order to reduce the colinearity of the task components.

Figure 2. Loadings dominating the encoding system. Dominant 5% of loadings are imaged in red and yellow. The importance of the system for each encoding and maintenance load condition is displayed in the bar graph. No negative loadings passed the 5% threshold for the encoding system, as reflected by the predictor weights displayed in Table 2. Coronal slices are located at the following MNI y axis coordinates: -94, -45, 1, 12, 33.

Figure 3. Loadings dominating the maintenance system. Dominant 5% of loadings are displayed. Positive loadings are imaged in red and yellow, and negative loadings are imaged in blue. The importance of the system for each encoding and maintenance load condition is displayed in the bar graph, as reflected by the predictor weights displayed in Table 2. Coronal slices are located at the following MNI y axis coordinates: -94, -45, -19, 28, 51.

Figure 1 (task description)
Click here to download high resolution image

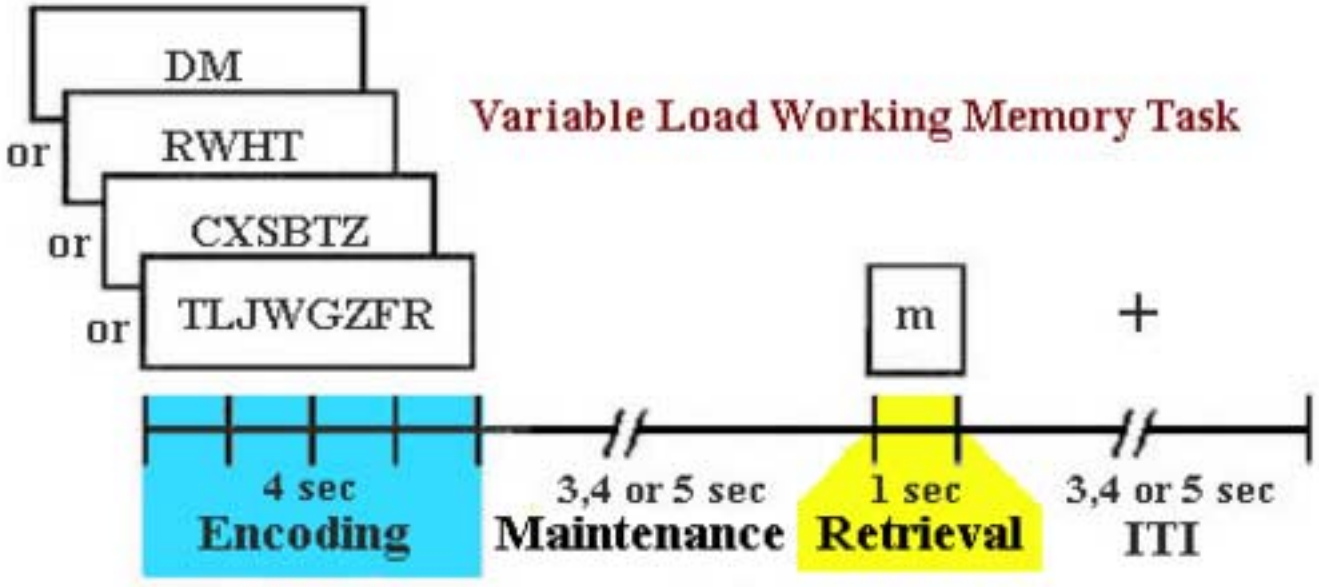

Figure 2 (encoding system)
Click here to download high resolution image

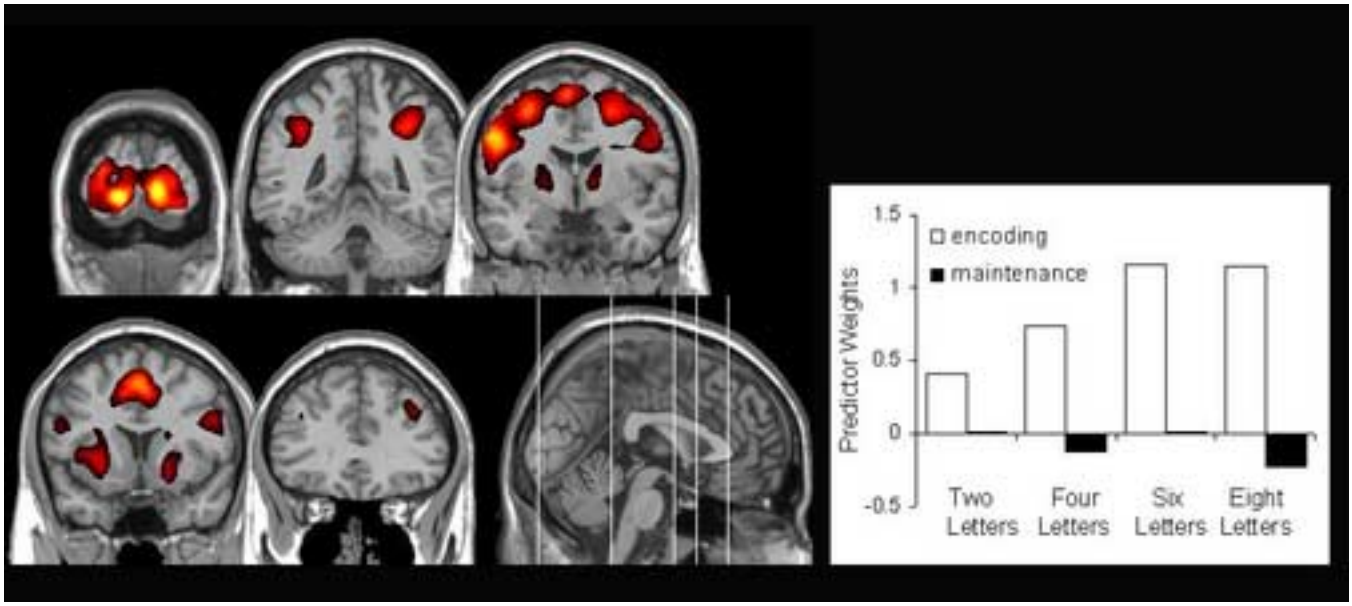

Figure 3 (maintenance system)
Click here to download high resolution image